Structural and functional characterization of barium zirconium titanate / epoxy composites

Filiberto González Garcia[1], César Renato Foschini[2], Jose Arana Varela[2], Elson Longo[2], Francisco Moura[1], Alexandre Zirpoli Simões[3]

[1]*Federal University of Itajubá - Unifei - Campus Itabira, Rua São Paulo 377, Bairro Amazonas, P.O. Box 355, 35900-37, Itabira, Minas Gerais, Brazil*
[2]*Chemistry Institute, Department of Chemistry-Physics, São Paulo State University, UNESP, 14800-900, Araraquara, São Paulo, Brazil*
[3]*Engineering Faculty, São Paulo State University, UNESP, 12516-410, Guaratinguetá, São Paulo, Brazil*

Abstract

The dielectric behavior of composite materials (barium zirconium titanate / epoxy system) was analyzed as a function of ceramic concentration. Structure and morphologic behavior of the composites was investigated by X-ray Diffraction (XRD), Fourier transformed infrared spectroscopy (FT-IR), Raman spectroscopy, field emission scanning electron microscopy (FE-SEM) and transmission electron microscopy (TEM) analyses. Composites were prepared by mixing the components and pouring them into suitable moulds. It was demonstrated that the amount of inorganic phase affects the morphology of the presented composites. XRD revealed the presence of a single phase while Raman scattering confirmed structural transitions as a function of ceramic concentration. Changes in the ceramic concentration affected Raman modes and the distribution of particles along into epoxy matrix. Dielectric permittivity and dielectric losses were influenced by filler concentration.

Keywords: composite materials, oxides, polymers, electron diffraction

I. Introduction

In recent years, there has been increased interest in high dielectric constant flexible particulate composites composed of a ferroelectric ceramic and polymer for high density energy storage and capacitor applications [1]. Usually, the dielectric constant of such polymer based composites is rather low (about 50) because of the lower dielectric constant of the matrix (usually below 10) [1–5]. For instance, in $BaTiO_3$/epoxy composites, although $BaTiO_3$ has a relatively high dielectric constant (>1000), the effective dielectric constant (ε_{eff}) of the composite was as low as 50, even when the highest possible concentration of ceramics was incorporated [2]. As the concentration of ceramics increases, unfortunately, the composite loses its flexibility. A new generation of high dielectric materials such as barium zirconium titanate ceramics (BZT) can be used in order to obtain composites with better performance. A number of theoretical studies and experimental observations have attempted to elucidate the remarkable (high) dielectric properties of BZT material. The interest in high strain piezoelectric materials increases for electromechanical transducers and various related applications [6]. Although the large family of lead-based perovskites and relaxors has shown great potential, lead-free compositions in these families will be of interest due to obvious future environmental concerns [7–12]. Modified $Ba(Zr,Ti)O_3$ has shown systematic changes in dielectric, piezoelectric, and phase transition characteristics in the bulk ceramic and single crystal forms [13]. In the paraelectric state, just above T_c, BZT ceramics are attractive candidates for dynamic random access memories and tunable dielectric devices. In this study, $Ba(Ti_{0.9}Zr_{0.10})O_3$ powders (BZT) were employed to produce the composite material which was chosen because it has improved dielectric and ferroelectric properties [14]. Usually, the

---

* Corresponding author: tel: +55 12 31232765
fax: +55 12 3123 2800, e-mail: *alezipo@yahoo.com*

preparation of the BZT phase by chemical routes have attracted wide attention including the hydrolysis of metal alkoxides, the polymeric precursor method derived from the Pechini method [14,15], and the co-precipitation of metal hydroxides and oxalates [16]. Although the chemical route facilitates the preparation of fine and homogeneous oxide powders with better reactivity and sinterability, its dielectric and ferroelectric properties are still very low. Alternatively, the solid-state reaction at 1200°C for 2 hours among the constituent $BaCO_3$, TiO_2 and, ZrO_2 can result in single phase BZT powders. This method is important to efficiently control ceramic properties due to its strong influence on the grain size and dielectric and ferroelectric properties by an oxygen interdiffusion, a chemical reaction, or structural defects in this particle size range. Measurements on dielectric permittivity as a function of temperature reveal anisotropic behaviour with a sharp phase transition which is indicative of a ferroelectric-relaxor behaviour [17–19].

Epoxy resins are being widely used in industrial applications such as adhesives and matrices for composite materials. High performances must be achieved through the synthesis and processing of the materials; in particular, good mechanical behaviour (stiffness and toughness) is expected. In previous studies, we evaluated the effects of an amine co-monomer on the thermal relaxations and mechanical properties [20]. The system of bisphenol A (diglycidyl ether) with aliphatic epoxide amine hardeners such as triethylenetetramine is extensively studied and reported in the literature [21,22]. In this research, the dielectric performance of BZT/epoxy matrix composites was studied to analyze dielectric behavior as a function of temperature and filler concentration. The aim of this investigation in a near future is to develop high density energy storage and capacitor devices by a careful control of modifying filler properties and a proper powder treatment to maximize the powder loading and dielectric properties.
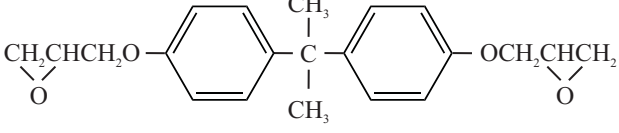
II. Experimental

Bisphenol A (diglycidyl ether) (DGEBA, DER 332) (Aldrich Brazil S.A) with an epoxy equivalent weight of 174 g·eq^{-1} determined by acid titration [23], was used as an epoxy prepolymer in all the epoxy formulations studied. The epoxy resin was degassed in a vacuum oven for 2 h at 80°C. Triethylenetetramine (TETA, tech. 60 % from ACROS, Brazil S.A.), was used as a curing agent, with an amine hydrogen equivalent weight of 26.8 g·eq^{-1}, determined by potentiometric titration in aqueous media [24]. Table 1 displays the structure and characteristics of the epoxy system employed in this study. $BaCO_3$ (Vetec, Brazil), ZrO_2 (Inlab, Brazil) and TiO_2 (Vetec, Brazil) (all analytical grade) were used. The curing agent and these compounds were used as received. $Ba(Ti_{0.9}Zr_{0.10})O_3$ (BZT) polycrystalline powders

were prepared by a mixed oxide method. All starting materials used were of analytical grade: $BaCO_3$ (Vetec, 99.99%), ZrO_2 (Inlab, 99.8%), TiO_2 (Vetec, 99.8%). These materials were ball milled in an alcohol medium for 24 hours in a polyethylene bottle, using zirconia balls. Then, the slurry was dried and thermally treated at 900°C in an air atmosphere for 12 hours.

The resulting powders were mixed in isopropyl alcohol by agitation at 6000 rpm for 5 minutes and the alcohol was eliminated by heating at 65°C until a constant weight was achieved. The powder was thermally treated at 1200°C for 120 minutes using a heating and a cooling rate of 5 °C/min. The powder was milled using a planetary mill with ZrO_2 balls (Fritsch, Pulverisette 7) for 90 minutes in isopropilic medium. The ceramic powders were added to the epoxy resin at different concentration and then suitably blended using an ultrasonic mixer (Sonic vibra-cell 150 W) for 10 min. The speed during preparation of composition ceramic powder/epoxy resin was 2000 rpm. The epoxy resin was mixed with the powder using different concentrations: 5, 10 and 15 phr (5, 10 and 15 g of filler per 100 g of DGEBA, respectively) before curing.

Epoxy composites were prepared by adding the curing agent to the epoxy resin mixture using the stoichiometric amount (epoxy ratio to amino-hydrogen e/a = 1). All formulations were mixed and degassed at room temperature under mechanical stirring for 15 min. The mixture was poured into polyethylene molds (cylindrical), cured in a forced air oven and cooled to room temperature. Each mixture was poured into glass moulds and cured at 100°C for 2 hours. The cure schedule was optimized by calorimetric studies to obtain fully cured networks. The glass transition temperature (T_g) of this system is 124°C [20]. XRD data were collected with a Rigaku Rint 2000 diffractometer under the following experimental condition: 50 kV, 150 mA, 20°≤ 2θ ≤ 80, $\Delta 2\theta$ = 0.02°, λCuK_α monochromatized by a graphite crystal, divergence slit of 2 mm, reception slit of 0.6 mm, step time of 10 s. Raman measurements were performed using an ISAT 64000 triple monochromator. An optical microscope was employed to focus the 514.5 nm radiation from a Coherent Innova 99 Ar + laser on the sample and to collect the back-scattered radiation. The scattered light dispersed by the spectrometer was detected by a charge-coupled device (CCD) detection system. FTIR spectra were recorded with a Bruker Equinox-55 instrument. Microstructural characterization was performed by FE-SEM (Supra 35-VP, Carl Zeiss, Germany) and transmission electron microscopy (TEM, Jeol 3010 URP). Samples were painted with a silver paste for dielectric measurements which were performed using a Hewlett Packard 4284A Impedance Analyser from 20 Hz to 1 MHz at room temperature. Dielectric permittivity and dielectric loss as a function of temperature were also measured.

Table 1. Structure and characteristics of the epoxy system monomers

Monomers	Formula	Supplier	M [g·mol^{-1}]	F
Triethylenetetramine (TETA)	H_2N-$(CH_2)_2$-NH-$(CH_2)_2$-NH-$(CH_2)_2$-NH_2	ACROS	146	6
Diglycidyl ether of bisphenol A (DGEBA)		Dow Chemical	~ 348 (174 g·eq^{-1})	2

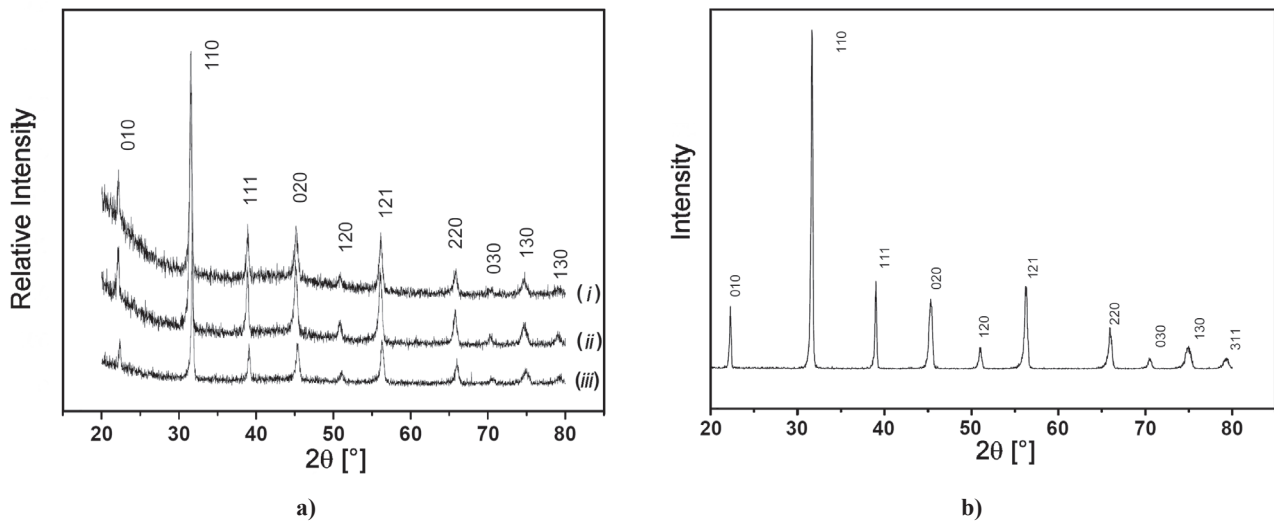M = molecular weight, F = functionality

Figure 1. X-ray data of: a) BZT/epoxy matrix composites with 5 (i), 10 (ii) and 15 phr (iii) and b) BZT powder

III. Results and discussion

The XRD pattern of the BZT/epoxy matrix composites with different ceramic concentrations is shown in Fig. 1a. X-ray reflections show that a single phase with a pseudo-cubic perovskite structure was obtained. In all systems investigated, Bragg reflections peaks are indicative of a perovskite structure which is character-ized mainly by a higher intense peak (hkl-110) at 2θ = 31° and no apparent peak splitting is identified. Independent of different filler amounts, Bragg reflections peaks reveal the formation of a stable solid solution between the epoxy system and the BZT lattice since no extra peaks appeared in the XRD pattern. For comparison, XRD pattern of pure BZT powder is shown in Fig. 1b. As can be seen, the room temperature XRD plot of $Ba(Ti_{0.9}Zr_{0.10})O_3$ powder crystallize into a single-phase perovskite structure. This is a clear indication that the addition of Zr is forming a stable solid solution with the $BaTiO_3$ lattice.
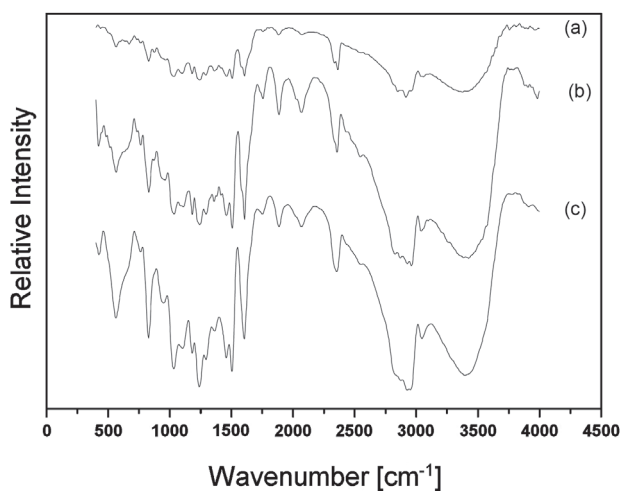
Figure 2 shows the FT-IR spectrum of a BZT/epoxy matrix composite with different ceramic concentrations. Regarding the ceramic structure, the main band characteristic of the oxygen-metal bond was observed in the region 450–640 cm^{-1} region. The vibrational mode located at around 1450 cm^{-1} is associated with an epoxy matrix related to methyl and methylene groups in the out-of-plane bending vibrational mode. Previous studies suggest that the absence of this band corresponds to a C=O relative to the powders which indicates that inorganic phases are free of carbonates [9]. This result is satisfactory from a technological point of view since of composite material properties depend on

Figure 2. FT-IR of BZT10/epoxy matrix composites with: a) 5, b) 10 and c) 15 phr

the powders properties used to prepare the two phase system. However, a vibrational band was observed that is associated with the deformation of O-H bonds near 3450 cm^{-1} which is attributed to stretching vibrations of composite O-H bonds. Regarding the epoxy matrix, the bands characteristic of this structure appear in the spectra [22]. The band around 3050 cm^{-1} is assigned to C-H stretching vibrational sp$_2$ bonds, and the bands around 2960, 2920 and 2880 cm^{-1} are associated with C-H stretching vibrational sp$_3$ bonds. The band at 2360 cm^{-1} indicates that the composite adsorbed CO$_2$ from the atmosphere. Bands associated with the aromatic ring appear around 1600, 1580, and 1500 cm^{-1}. The band around 1020 cm^{-1} is associated with C-O-C ether groups while the band around 1250 cm^{-1} is associated with C-N stretching vibration. The bands at 1360 and 1375 cm^{-1} can be assigned to methyl group bonds between the carbon aromatic ring and the band at 828 cm^{-1} which is assigned to the 1.4 substitution. The absence of a band around 900 cm^{-1}, which is associated to epoxy groups, indicates that the epoxy system has attained a high conversion. Although relative transmittance values increase with an increase in the amount of filler, no extra bands appeared in the spectrum which indicates the formation of a stable solid solution between the epoxy matrix and the BZT lattice. The increase in epoxy peaks intensity as the ceramic content increases indicates that the mixing process of filler and epoxy resin was carried out for only few minutes and resulted in a non-homogeneous oxide distribution in the epoxy matrix.

Room temperature Raman spectra are displayed in Fig. 3. Because of the random grain orientations in the powders evidenced by SEM and not shown in the text, the directions of the phonon wave vectors are randomly distributed from one grain to another with respect to the crystallographic axes. The evolution of Raman spectra with ceramic concentration shows some interesting changes. As observed, at increased ceramic concentration, the Raman line at 123 cm^{-1} is absent. Taking the mass ratio Zr/Ti = 1.9 into consideration this mode frequency is expected to be about 129 cm^{-1} for Zr replacing Ti sites which will be further reduced by an increase in the ionic radius [R (Ti^{4+}) = 0.0745 nm, R (Zr^{4+}) = 0.086 nm]. The additional mode could therefore be associated with a normal mode involving Zr atoms. Since this mode disappears with a more concentrated amount of ceramic, it may be considered as an indication of short range structural disordering. These observations could not be observed in the X-ray studies due to the different coherence length and time scale involved in the process. The modes further split into longitudinal (LO) and transverse (TO) components due to long electrostatic forces associated with lattice ionicity, which are caused by Ba^{2+} ions in BaTiO$_3$ such as reported for the Ba(Zr$_{0.10}$Ti$_{0.90}$)O$_3$ lattice [25,26]. The

spectrum shows the stretching mode of A1(TO1) and A1(TO3) at around 193 and 517 cm^{-1}, according to the references [27,28]. The E1(TO1) and E1(TO2) modes that are associated with the tetragonal-cubic phase transition were observed at 116 and 301 cm^{-1}, whereas the A1(LO3) mode was found at 720 cm^{-1}, with zirconium (Zr) substituted at the titanium (Ti) sites. However, the coupling between the sharp A1(TO1) and broad A1(TO2) modes reduces as the intensity of the A1(TO2) mode decreases [29,30].

A SEM analysis of a BZT/epoxy matrix composite is shown in Fig. 4a-c. For comparison, SEM figure of epoxy matrix was presented. An increase in the agglomerates size was observed as the amount of ceramic powder increases. The agglomerates are rounded in form which is typical for the mixed oxide method. Regions without filler or trails of micro-porosity are observed as are particles with a low size and a relative fine size distribution. In all samples, particle agglomeration results from a non-homogeneous dispersion of particles during the mixing step. It is clear that mixing in a mortar and pestle generates a simple mixture where the components could be identified separately. Although particle agglomeration exists, our data reveal that the inorganic phase and epoxy matrix are homogeneously distributed in the particle. An intimate mixing of the barium zirconium titanate and the epoxy matrix yields a composite which suggests that the composite actually consists of fine agglomerates composed of an oxide on the epoxy matrix. The BZT/epoxy matrix composite with 10 phr consists of more homogeneous surface morphology (Fig. 4b). SEM micrograph of epoxy resin reveals a continuous phase with smooth areas indicating larger solubility of the modifiers and a complete polymerization rate.

TEM analyses of the BZT/epoxy matrix composite with 10 phr is illustrated in Fig. 5. A closer look at the darker part (bottom left-A) reveals that it is actually an agglomerate composed of a large number of par-
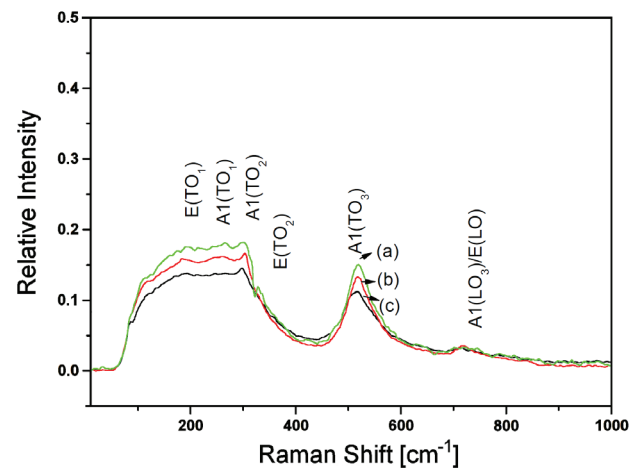

Figure 3. Raman analyses of BZT10/epoxy matrix composites with (a) 5, (b) 10 and (c) 15 phr
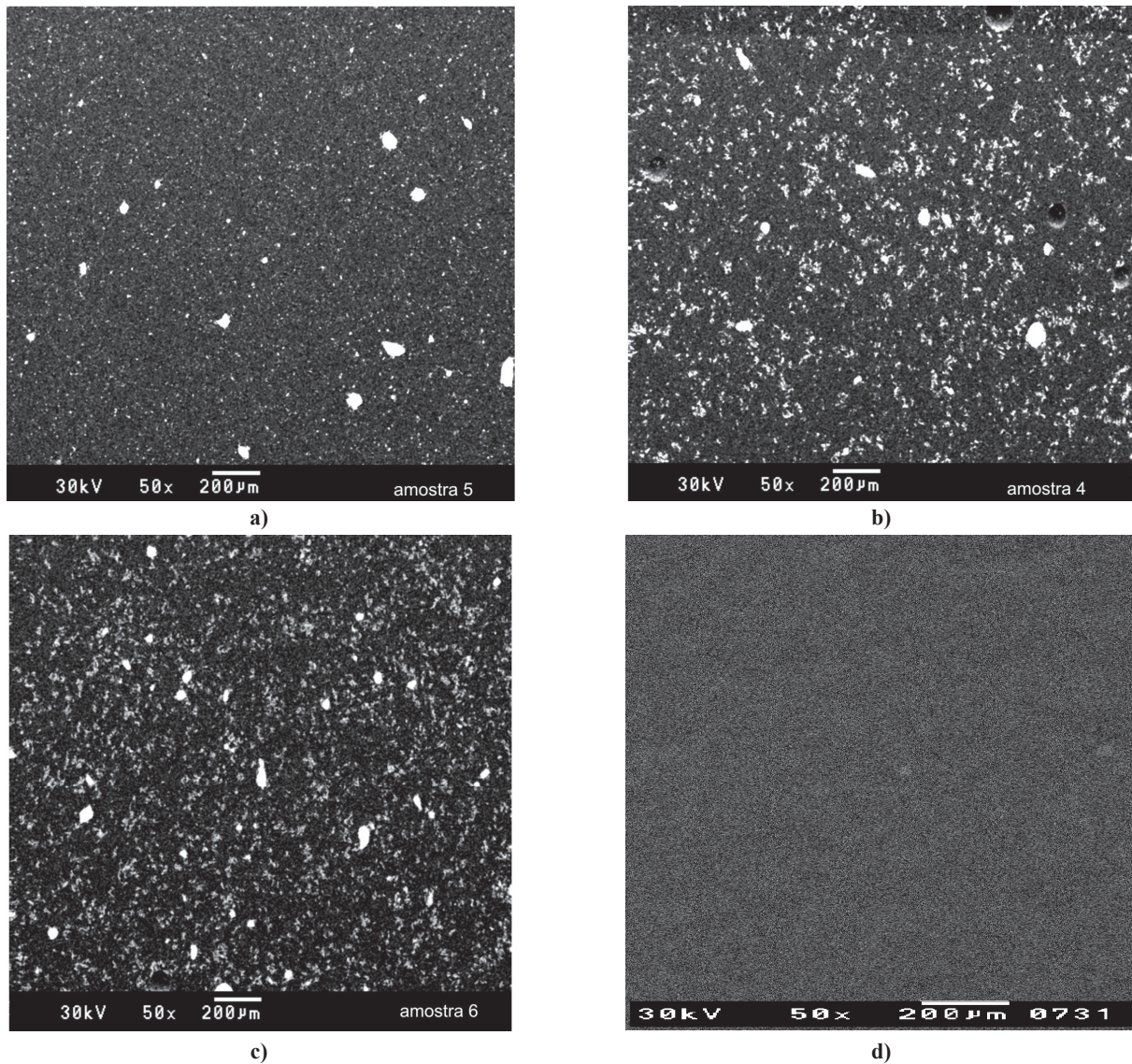
Figure 4. SEM micrographs of BZT10/epoxy matrix composites with (a) 5, (b) 10, (c) 15 phr and (d) SEM micrography of pure epoxy matrix
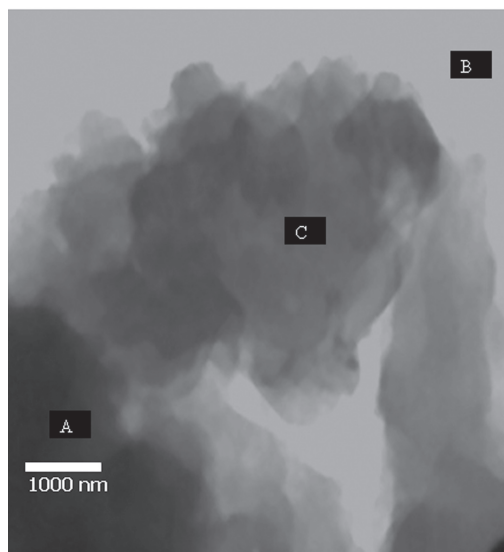

Figure 5. TEM micrograph of BZT10/epoxy matrix composite with 10 phr evidencing (A) agglomerate of particles, (B) epoxy matrix and (C) composite

ticles while white regions are believed to be the epoxy matrix (top-B). The inorganic phase and the epoxy matrix can be clearly distinguished. The darker part corresponds to barium zirconium titanate as confirmed by a further magnification which indicates randomly grown crystallites. The epoxy matrix is visible at the bottom (center) and the top of the image while part of a structured oxide is located at the left. It is clear that an intimate mixing of the barium zirconium titanate and the epoxy matrix yields a composite (center-C). The mixing of an inorganic phase and epoxy system is desirable to achieve good end-use properties and a better composite efficiency. It is possible that the composites may also provide better pathways for ion diffusion and lower ionic resistance during the charge-discharge process which is useful for dynamic random access memory (DRAM) applications.

The temperature dependence of dielectric permittivity is shown in Fig. 6a. The dielectric permittivity
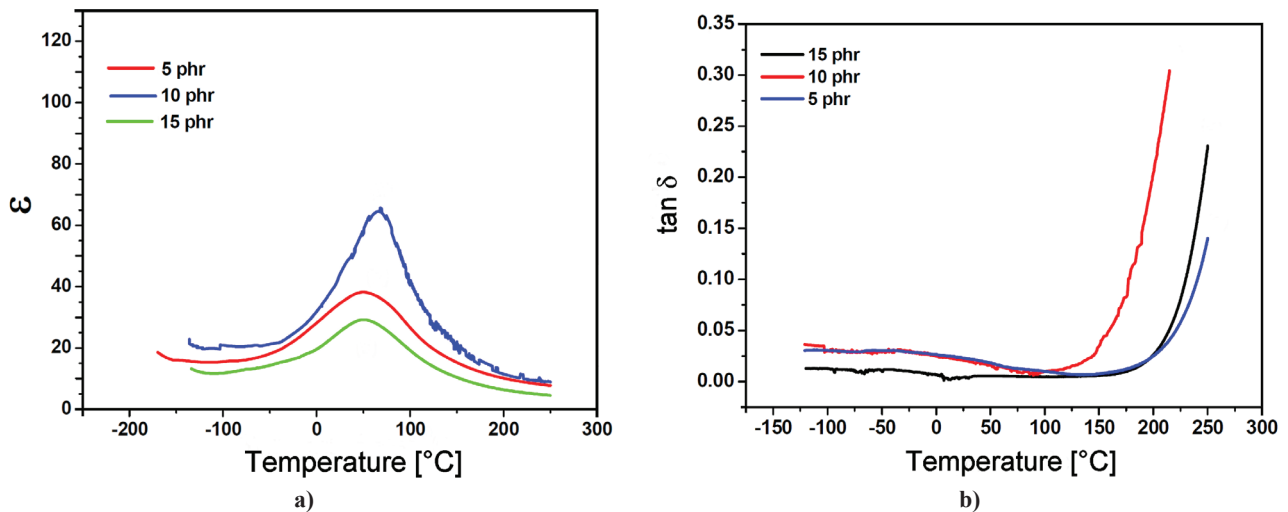
Figure 6. Temperature dependence of dielectric permittivity (a) and dielectric loss (b) at 10 KHz for BZT10/epoxy matrix composites with 5, 10 and 15 phr

measured at 10 kHz are 36, 66 and 28 while the dielectric losses are 0.13, 0.30 and 0.22 for 5, 10 and 15 phr, respectively. For a 10 phr composite, the phase transition is observed at 66°C, and its maximum dielectric permittivity (ε_m) reaches 66. In this sample, a structural phase transition occurs which corresponds to the transition of a paraelectric (cubic) to ferroelectric (tetragonal) phase (at T_c). The dielectric permittivity increases gradually with an increase in temperature up to the transition temperature (T_c) or Curie point and then decreases. Also, the maximum dielectric permittivity (ε_m) and the corresponding maximum temperature, (T_m), depend on the ferroelectric ceramic concentration. The magnitude of the dielectric permittivity decreases in this case, and the Curie temperature shifts toward a lower temperature which indicates that dielectric polarization is a relaxation type in nature. The region around the dielectric peak is broadened due to a disorder in the cations arrangement in one or more crystallographic sites of the structure [31,32]. The reduction

of dielectric permittivity with 15 phr indicates that filler agglomerates are deleterious for the improvement of composite properties. For the epoxy matrix, the relative dielectric permittivity remains around 5.7 and the dielectric loss is 0.018 at 25°C [33]. Figure 6b shows the temperature dependence of dielectric loss determined at 10 KHz. The dielectric loss is almost temperature independent, although it also presents a very small peak just below T_c. At lower temperatures, a small temperature dependence of dielectric loss was observed with stabilization at elevated temperatures. The possible formation of metal vacancies may result in a reduced dielectric loss at elevated temperatures and reflects that good insulation resistance was maintained at high temperatures which is important in the development of high density energy storage and capacitor devices. In addition, the dielectric loss was much lower than the dielectric loss of pure *BZT* ceramics reported in our previous work [34] which is attributed to the decrease in space charge density as the epoxy resin is in-
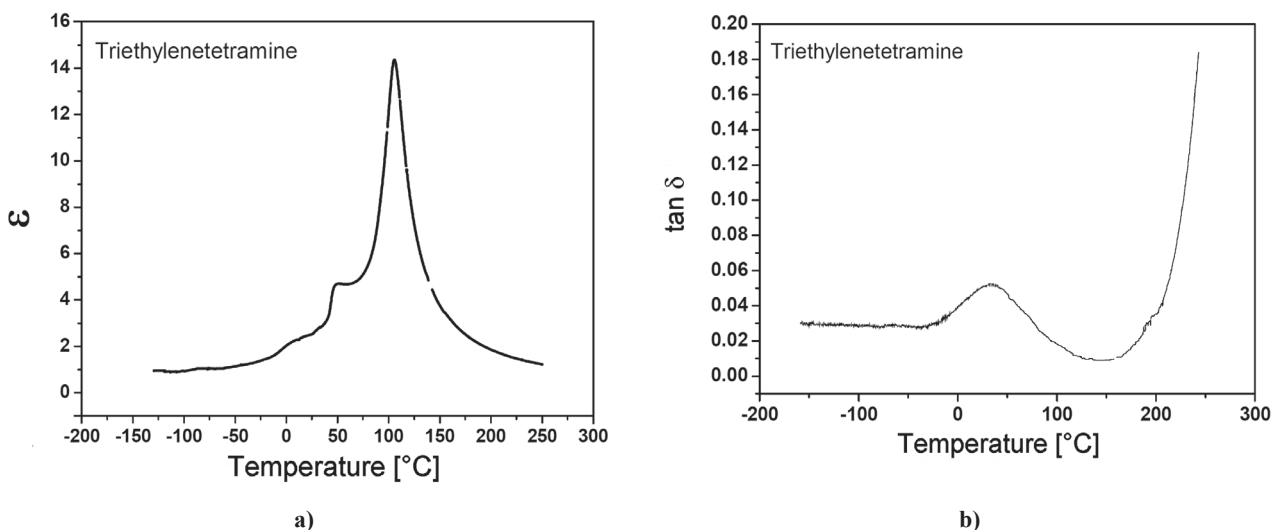

Figure 7. Temperature dependence of dielectric permittivity (a) and dielectric loss (b) at 10 kHz for triethylenetetramine

corporated in the BZT lattice. The higher value of dielectric loss at elevated temperatures may be due to the transport of ions with higher thermal energy. The sharp increase in dielectric loss may be due to the scattering of thermally activated charge carriers and the presence of defects. At higher temperatures the conductivity begins to dominate, which in turn is responsible for the rise in dielectric loss that is associated with conduction loss. Also, at a high temperature (paraelectric phase) the contribution of ferroelectric domain walls to dielectric loss decreases. Chahal *et al.* [33] reported dielectric permittivity of 39 and 22 for 55 vol% ceramic/polyacrylonitrile and for the 50% ceramic/polynorbornene composites, respectively. Bhattacharya *et al.* [35] reported dielectric permittivity of 9 and 34 for two kinds of PWB- compatible composites at a filler loading of 21 and 46%, respectively. The dielectric permittivity of 66 with a filler loading of 10 phr in this study thus compares favorably with these literature data. The changes which occur in the dielectric loss are due to extrinsic resonance behaviour which may be caused by defects (vacancy, movable ion, leaky grain boundary, etc.) that developed in the structure of the bulk material with donor dopants [36–46].

The temperature dependence of dielectric permittivity is shown in Fig. 7a for the triethylenetetramine. The dielectric permittivity measured at 10 kHz is 14 while the dielectric losses are 0.016, respectively. The dielectric permittivity increases gradually with an increase in temperature up to the transition temperature (T_c) or Curie point and then decreases. The rise in dielectric loss at higher temperatures is associated with the conductivity which in turn is responsible for loss values. Changes in the permittivity values as a function of temperature are attributed to dielectric relaxations which are more pronounced at higher temperatures due to the micro-Brownian motion of the whole chain (segmental movement). Nevertheless, these changes are also affected by the interfacial polarization process known as Maxwell-Wagner-Sillar, which exists in heterogeneous dielectric materials and is produced by the traveling of charge carriers [47]. Relaxations peaks were influenced by the interfacial polarization effect which generates electric charge accumulation around the polymeric chain and the displacement of charges around it [48].

IV. Conclusions

Single phase BZT composite materials were obtained using a mixed oxide method. The structure and morphologic behavior of an epoxy system/barium zirconium titanate powder was analyzed as a function of ceramic concentration that revealed a perovskite structure with rounded agglomerates which is typical for the mixed oxide method. Raman spectroscopy indicated a change in the crystal structure with an increase in

the ceramic concentration which indicated short-range structural disordering. TEM analyses confirmed an intimate mixing of the barium zirconium titanate and the epoxy matrix to produce a composite. The inorganic phase consists of randomly grown crystallites while the epoxy matrix is viewed as the most of structured composite. Low porosity and better homogeneous size distribution is evident for the BZT/epoxy matrix composite with 10 phr. The dielectric permittivity was influenced by the filler concentration volume because particle distribution is the most important parameter which affects composite permittivity values. To obtain the best dielectric properties of ceramic BZT/epoxy composites, proper powder treatment is required to maximize the powder loading and dielectric properties by carefully controlling the particle size, phase content and elimination of constraint forces from neighboring grains.

References

1. Y.J. Li, M. Xu, Z.M. Dhang, "Dielectric behavior of a metal-polymer composite with low percolation threshold", *Appl. Phys. Lett.*, **89** (2006) 072902-072904.
2. D-H. Kuo, C-C. Chang, T-Y. Su, W-K. Wang, B-Y. Lin, "Dielectric behaviours of multi doped BaTiO$_3$/epoxy composites", *J. Eur. Ceram. Soc.*, **21** (2001) 1171–1177.
3. R. Gregório, J.M. Cestari, F.E. Bernardino, "Dielectric behaviour of thin films of β-PVDF/PZT and β-PVDF/BaTiO$_3$ composites", *J. Mater. Sci.*, **11** (1996) 2925–2930.
4. H.L.W. Chan, W.K. Chan, Y. Zhang, C.L. Choy, "Pyroelectric and piezoelectric properties of lead titanate/polyvinylidene fluoride-trifluoroethylene 0-3 composites", *IEEE Trans. Dielectr. Electr. Insul.*, **4** (1998) 505–512.
5. C.J. Dias, D.K. Das-Gupta, "Inorganic ceramic/polymer ferroelectric composite electrets", *Dielectr. Electr. Insul.*, **5** (1996) 706–734.
6. Z.Yu, R. Yu, A.S. Bhalla, "Dielectric behavior of Ba(Ti$_{1-x}$Zr$_x$)O$_3$ single crystals", *J. Appl. Phys.*, **88** (2000) 410–415.
7. Z. Yu, C. Ang, R. Guo, A.S. Bhalla, "Dielectric properties and high tunability of Ba(Ti$_{0.7}$Zr$_{0.3}$)O$_3$ ceramics under dc electric field", *Appl. Phys. Lett.*, **81** (2002) 1285–1287.
8. A. Dixit, S.B. Majumder, R.S. Katiyar, "Relaxor behavior in sol-gel-derived BaZr(0.40)Ti(0.60)O$_3$ thin films", *Appl. Phys. Lett.*, **82** (2003) 2679–2681.
9. P.S. Dobal, R.S. Katiyar, "Studies on ferroelectric perovskites and Bi-layered compounds using micro-Raman spectroscopy", *J. Raman. Spectrosc.*, **33** (2002) 405–423.

10. A. Dixit, S.B. Majumder, A. Savvinov, R.S. Katiyar, R. Guo, A.S. Bhalla, "Investigations on the sol-gel-derived barium zirconium titanate thin films", *Mater. Lett.*, **56** (2002) 933–940.

11. D.S. Paik, S.E. Park, S. Wada, S.F. Liu, T.R. Shrout, "*E*-field induced phase transition<001>-oriented rhombohedral $0.92Pb(Zn_{1/3}Nb_{2/3})O_3$–$0.08PbTiO_3$ crystals", *J. Appl. Phys.*, **85** (1999) 1080–1083.

12. D. Hennings, H. Schell, "Diffuse ferroelectric phase-transitions in Ba(Diffuse ferroelectric phase-transitions in $Ba(Ti_{1-y}Zr_y)O_3$ ceramics", *J. Am. Ceram. Soc.*, **65** (1982) 539–544.

13. Mc Quarrie, F.W. Behnke. "Structural and dielectric studies in the system $(Ba, Ca) (Ti, Zr)O_3$", *J. Am. Ceram. Soc.*, **37** (1954) 539–543.

14. F. Moura, A.Z. Simões, L.S. Cavalcante, M.A. Zaghete, J.A. Varela, "Influence of tungsten dopant on sintering and Curie temperatures of $Ba(Zr_{0.10}Ti_{0.90})O_3$ ceramics", *Ferroelectrics*, **367** (2008) 120–130.

15. M.P. Pechini, "Method of preparing lead and alkaline earth titanates and niobates and coating method using the same to form a capacitor", *US Patent 3330697*, 11 July (1967).

16. M.A. Zaghete, C.O. Paiva-Santos, J.A. Varela, E. Longo, Y.P. Mascarenhas, "Phase characterization of lead zirconate titanate obtained from organic solutions of citrates", *J. Am. Ceram. Soc.*, **75** (1992) 2088–2093.

17. J. Choy, Y. Han, S. Kim, "Oxalate coprecipitation route to the piezoelectric. $Pb(Zr, Ti)O_3$ oxide", *J. Mater. Chem.*, **7** (1997) 1807–1813.

18. F. Moura, A.Z. Simões, E.C. Aguiar, I.C. Nogueira, M.A. Zaghete, J.A. Varela, E. Longo, "Dielectric investigations of vanadium modified barium titanate zirconate ceramics obtained from mixed oxide method", *J. Alloys Compds.*, **479** (2009). 280–283.

19. F. Moura, A.Z. Simões, B.D. Stojanovic, M.A. Zaghete, J.A. Varela, E. Longo, "Dielectric and ferroelectric characteristics of barium zirconate titanate ceramics prepared from mixed oxide method", *J. Alloys. Comp.*, **462** (2008) 129–134.

20. F. González Garcia, M.E. Leyva, M.C. Oliveira, A.A.A. Queiroz, A.Z. Simões, "Influence of chemical structure of hardener on mechanical and adhesive properties of epoxy polymers", *J. Appl. Polym. Sci.*, **117** (2010) 2213–2219.

21. C.A. May, *Epoxy Resins. Chemistry and Technology*, New York, Marcel Dekker. 1988.

22. H. Lee, K. Neville, *Handbook of Epoxy Resins*, New York, McGraw-Hill & Inc. 1967.

23. F. González Garcia, P.M. Da Silva, B.G. Soares, J. Rieumont, "Combined analytical techniques for the determination of the amine hydrogen equivalent weight in aliphatic amine epoxide hardeners", *Polym. Test.*, **26** (2007) 95–101.

24. A. Chaves, R.S. Katiyar, S.P.S. Porto, "Coupled modes with A_1 symmetry in tetragonal $BaTiO_3$", *Phys. Rev. B.*, **10** (1974) 3522–3533.

25. P.S. Dobal, A. Dixit, R.S. Katiyar, Z. Yu, R. Guo, A.S. Bhalla, "Micro-Raman scattering and dielectric investigations of phase transition behavior in the $BaTiO_3$–$BaZrO_3$ system", *J. Appl. Phys.*, **89** (2001) 8085–8091.

26. J. Kreisel, P. Bouvier, M. Maglione, B. Dkhil, A. Simon, "High-pressure Raman investigation of the Pb-free relaxor $BaTi_{0.65}Zr_{0.35}O_3$", *Phys. Rev. B,* **69** (2004) 092104–092107.

27. B.D. Begg, K.S. Finnie, E.R. Vance, "Raman study of the relationship between room-temperature tetragonality and the curie point of barium titanate", *J. Am. Ceram. Soc.*, **79** (1996) 2666–2672.

28. P.S. Dobal, A. Dixit, R.S. Katiyar, Z. Yu, R. Guo, A.S. Bhalla, "Micro-Raman scattering in Nb_2O_5-TiO_2 ceramics", *J. Raman. Spectrosc.*, **33** (2002) 121–124.

29. A. Dixit, S.B. Majumder, P.S. Dobal, R.S. Katiyar, A.S. Bhalla, "Phase transition studies of sol-gel deposited barium zirconate titinate thin films", *Thin Solid Films*, **447** (2004) 284–287.

30. L. Ramajo, M. Reboredo, M. Castro, "Dielectric response and relaxation phenomena in composites of epoxy resin with $BaTiO_3$ particles", *Composites Part A.*, **36** (2005) 1267–1274.

31. M.E. Lines, A.M. Glasss, *Principles and applications of ferroelectrics and related materials*, Oxford University Press, Oxford 1977.

32. Y. Wu, S.J. Limmer, T.P. Chou, C. Nguyen, C. Guozhong, "Influence of tungsten doping on dielectric properties of strontium bismuth niobate ferroelectric ceramics", *J. Mater. Sci. Lett.*, **21** (2002) 947–949.

33. P. Chahal, R.R. Tummala, "A novel integrated decoupling capacitor for MCM-L technology", *IEEE Trans. Comp. Packag. Manufact. Technol.*, **B 21** (1998) 184–193.

34. A.Z. Simões, C.S. Riccardi, A.H.M. Gonzalez, A. Ries, E. Longo, J.A. Varela, "Piezoelectric properties of $Bi_4Ti_3O_{12}$ thin films annealed in different atmospheres", *Mater. Res. Bull.*, **42** (2007) 967–974.

35. S. Bhattacharya, R.R. Tummala, P. Chahal, G. White, pp. 68–70 in *International Symposium on Advanced Packaging Materials*, Atlanta, USA, 1997.

36. A.Z. Simões, M.P. Cruz, A. Ries, E. Longo, J.A. Varela, R. Ramesh, "Ferroelectric and piezoelectric properties of bismuth titanate thin films grown on different bottom electrodes by soft chemical solution and microwave annealing", *Mater. Res. Bull.*, **42** (2007) 975–981.

37. A.Z. Simões, E.C. Aguiar, A. Ries, E. Longo, J.A. Varela, "Niobium doped $Bi_4Ti_3O_{12}$ ceramics obtained by the polymeric precursor method", *Mater. Lett.*, **61** [2] 2007, 588–591.

38. L.S. Cavalcante, A.Z. Simões, L.P.S. Santos, M.R.M.C. Santos, E. Longo, J.A. Varela, "Dielectric properties of $Ca(Zr_{0.05}Ti_{0.95})O_3$ thin films prepared by chemical solution deposition", *J. Solid State Chem.*, **179** (2006) 3739–3743.

39. A.Z. Simões, M.A. Ramírez, B.D. Stojanovic, E. Longo, J.A. Varela, "The effect of microwave annealing on the electrical characteristics of lanthanum doped bismuth titanate films obtained by the polymeric precursor method", *Appl. Surf. Sci.*, **252** (2006) 8471–8475.

40. A.Z. Simões, S. Cava, L.S. Cavalcante, M. Cilense, E. Longo, J.A. Varela, "Ferroelectric and dielectric properties of $Ba_{0.5}Sr_{0.5}(Ti_{0.80}Sn_{0.20})O_3$ thin films grown by the soft chemical method", *J. Solid State Chem.*, **179** (2006) 2972–2976.

41. A.Z. Simões, M.A. Ramírez, E. Longo, J.A. Varela, "Leakage current behavior of $Bi_{3.25}La_{0.75}Ti_3O_{12}$ ferroelectric thin films deposited on different bottom electrodes", *Mater. Chem. Phys.*, **107** (2008) 72–76.

42. L.S. Cavalcante, A.Z. Simões, M.O. Orlandi, M.R.M. C. Santos, J.A. Varela, E. Longo, "Dependence of annealing time on structural and morphological properties of $Ca(Zr_{0.05}Ti_{0.95})O_3$ thin films", *J. Alloys Compd.*, **453** (2008) 386–391.

43. D.P. Volanti, D. Keyson, L.S. Cavalcante, A.Z. Simões, M.R. Joya, E. Longo, J.A. Varela, P.S. Pizani, A.G. Souza, "Synthesis and characterization of CuO flower-nanostructure processing by a domestic hydrothermal microwave", *J. Alloys Compd.*, **459** (2008) 537–542.

44. A.Z. Simões, M.A. Ramirez, C.S. Riccardi, E. Longo, J.A. Varela, "Effect of the microwave oven on structural, morphological and electrical properties of $Sr-Bi_4Ti_4O_{15}$ thin films grown on $Pt/Ti/SiO_2/Si$ substrates by a soft chemical method", *Mater. Character.*, **59** (2008) 675–680.

45. D. Keyson, D.P. Volanti, L.S. Cavalcante, A.Z. Simões, J.A. Varela, E. Longo, "CuO urchin-nanostructures synthesized from a domestic hydrothermal microwave method", *Mater. Res. Bull.*, **43** (2008) 771–775.

46. M. Zhang, Z. Jin, J. Zhang, X. Gou, J. Yang, X. Wang, Z. Zhang, "Effect of annealing temperature on morphology, structure, and photocatalytic behavior of nanotubed $H_2Ti_2O_4(OH)_2$", *J. Mol. Catal. A: Chem.*, **217** (2004) 203–210.

47. G. Psarras, E. Manolakaki, G.M. Tsangaris, "Electrical relaxations in polymeric particulate composites of epoxy resin and metal particles", *Composites Part A.*, **33** (2002) 375–384.

48. G. Tsangaris, N. Kouloumbi, S. Kyvelidis, "Interfacial relaxation phenomena in particulate composites of epoxy resin with copper or iron particles", *Mater. Chem. Phys.*, **44** (1996) 245–250.